Genes & Diseases (2023) 10, 727–730

Available online at www.sciencedirect.com

ScienceDirect

journal homepage: www.keaipublishing.com/en/journals/genes-diseases

RAPID COMMUNICATION

Comparison analysis of multiple-omics data between female germline stem cells and spermatogonial stem cells

Female germline stem cells (FGSCs) and spermatogonial stem cells (SSCs) are germline stem cells that transmit the genetic material from generation to generation. Hence, it is essential to understand the similarities and differences between FGSCs and SSCs. In this study, we comprehensively compared the epigenetics of FGSCs and SSCs, including high-order chromatin organization, chromatin histone modification, and transcriptome by analyzing multiple-omics data (Hi-C, ChIP-seq, and RNA-seq). We found that FGSCs and SSCs had both similar and different chromatin histone modifications that were correlated with their chromatin organization. We also identified cell-specific enhancer–promoter interactions in FGSCs and SSCs. Furthermore, we found that the X chromosome was similar in FGSCs and SSCs by principal component analysis of the X chromosome. By using RNA fluorescence in situ hybridization (RNA FISH) to confirm the inactivation of the X chromosome in FGSCs, we compared the high-order chromatin structure between activated and inactivated X chromosomes in FGSCs. In summary, we performed a systematic comparison analysis of the epigenetics between FGSCs and SSCs from multiple perspectives using multiple-omics data.

To determine the similarities and differences in epigenetics (histone modification and chromatin structure) between FGSCs and SSCs, we firstly interactively analyzed the published Hi-C, ChIP-seq and RNA-seq data of FGSCs and SSCs to explore their relationships.[1–3] We examined the PC1 score of the eigenvector of Hi-C contact maps between FGSCs and SSCs at 400-kb resolution, where positive and negative PC1 values represented A and B compartments, respectively. Spearman's correlation analysis showed that H3K27ac and H3K4me3 were highly correlated with compartment status in both the FGSCs and SSCs (Fig. S1A). In the Integrative Genomics Viewer (IGV) browser, H3K27ac and H3K4me3 in chr19:40 Mb–60Mb were shown to be highly enriched in compartment A but not in compartment B (Fig. S1B), suggesting chromatin histone modification was correlated with the compartment status of the chromatin structure. Next, we examined the signals of histone medication in the switch compartment (FGSCs switch to SSCs). The result showed that H3K4me3 and H3K27ac were significantly different in the switch compartment of FGSCs compared with their status in the stable compartment (Fig. S1C). By analyzing the identified TAD boundaries between FGSCs and SSCs, we found H3K4me3, H3K27me3, and H3K27ac were highly enriched in the TAD boundaries, consistent with the higher gene expression in the TAD boundaries (Fig. S1D). These results indicated that histone modification was correlated with high-order chromatin structure, implying they could work together to regulate gene expression. Next, we detected chromatin loops in FGSCs and SSCs and identified enhancer-promoter interactions that were enriched by H3K4me3 and H3K27ac. By building the interaction networks with a modularity algorithm, we classified those interactions into three subsets: FGSC-specific, SSC-specific and GSC-shared (Fig. 1A). Interestedly, most communities displayed a promoter was interacted with multi-enhancers, indicating that enhancers contributed to the gene expression. RNA-seq showed the genes located in the specific enhancer-promoter interactions have higher expression than GSC-shared (Fig. 1B), suggesting the distinct formation of enhancer-promoter interactions in FGSC or SSC would regulate the gene expression. Then, the K-means clustering of ChIP-Seq signals divided them into four major classes on active promoter (H3K4me3) and enhancer (H3K27ac) sites (Fig. 1C; Fig. S2). The GO enrichment analysis showed that cluster 2 of active enhancers were enriched in reproductive processes such as sex differentiation, sexual reproduction, and reproductive development (Fisher's exact test, $P < 0.05$) (Fig. 1C; Fig. S2). These enhancer-promoter interactions

Peer review under responsibility of Chongqing Medical University.

https://doi.org/10.1016/j.gendis.2022.09.003

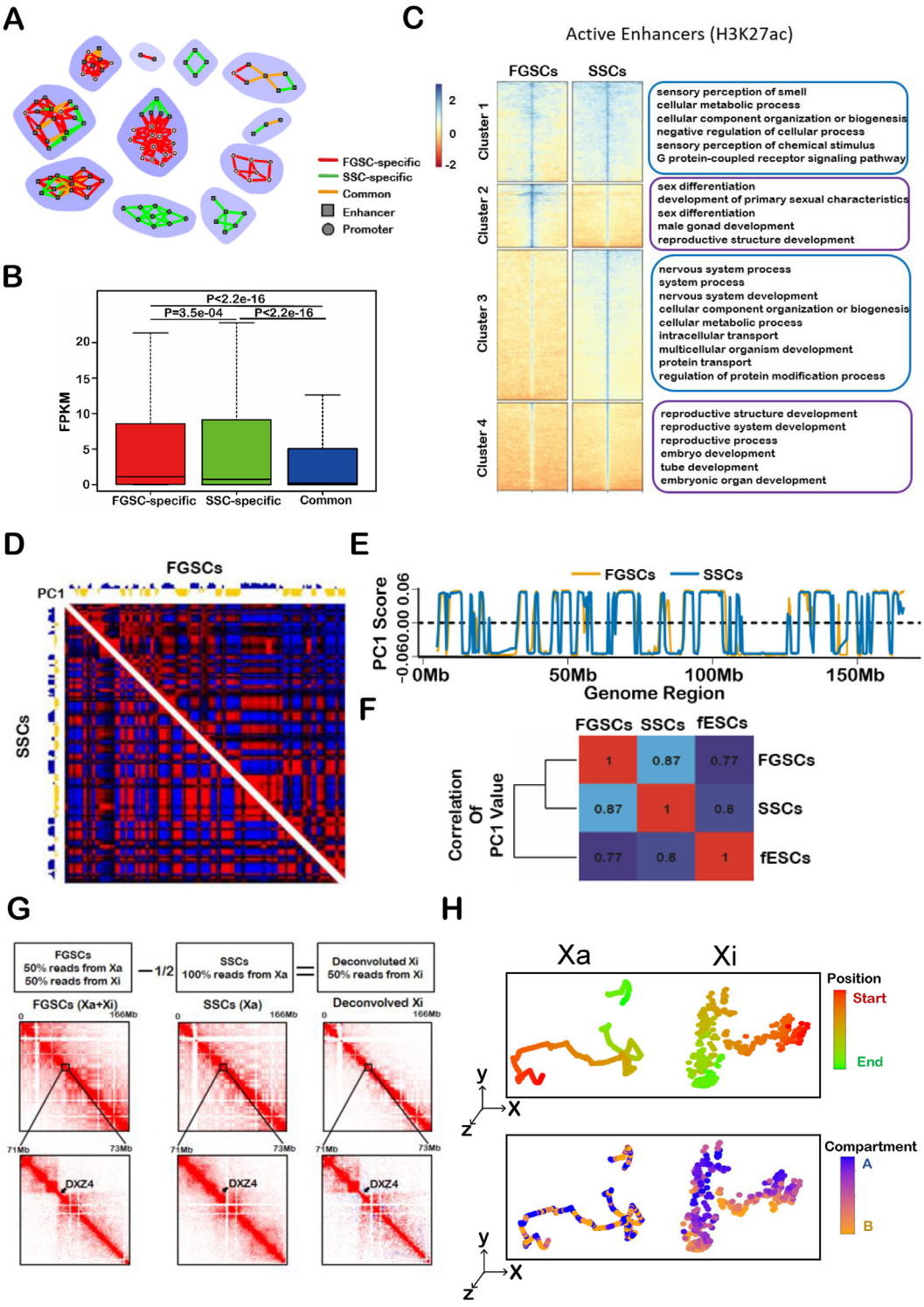

Figure 1 The similarity and differences of epigenetics between FGSCs and SSCs. **(A)** The communities of Enhancer-Promoter interactions. Circles indicate promoters and squares indicate enhancers. **(B)** The expression of genes located in Enhancer-Promoter interactions. **(C)** K-means clustering of H3K27ac ChIP-seq data at enhancer—promoter interaction regions in FGSCs and SSCs. **(D)** Pearson's correlation heat map showing the similarity between the X chromosome structure in FGSCs and SSCs. **(E)** First principal component (PC1) values for the X chromosome in FGSCs and SSCs. **(F)** Spearman's correlation of PC1 values for the X chromosome in FGSCs, SSCs, and fESCs. **(G)** Deconvolution of the Xi signal from Hi-C data obtained in FGSCs (Xa + Xi) by subtracting the Xa contribution estimated from SSCs. A small region containing the DXZ4 macrosatellite showed two domains in FGSCs and deconvoluted Xi, but not in SSCs. Blue pixels indicate negative values; red pixels indicate positive values. **(H)** The 3D physical model of the X chromosome. Top: the 3D model of Xa and Xi; Bottom: the 3D chromosomal model colored by A/B compartment status in Xa and Xi.

were divided into two subsets: FGSCs lost and FGSCs gained (Fig. S3). Overall, these findings indicate that FGSCs and SSCs had both similar and different chromatin histone modifications that were correlated with their chromatin organization to regulate gene expression.

During mammalian development, one of the female X chromosomes is randomly inactivated to ensure matched dosages in males and females.[4] To dissect the high-order organization of the X chromosome in FGSCs and SSCs, we performed Pearson's correlation analysis of the Hi-C matrix in the X chromosome. The results show that FGSCs and SSCs were strongly correlated (Fig. 1D). Furthermore, when we extracted the eigenvectors of the chromosome interactions and used the PC1 score to compare the structure of the X chromosome in FGSCs and SSCs, we found that the X chromosomes in FGSCs and SSCs were similar (Pearson's correlation = 0.87) (Fig. 1E). By comparison, we found that the autosomes FGSCs and SSCs had lower correlation scores (mean correlation = 0.21) (Fig. S4), suggesting that the similarity of chromatin architecture of the X chromosomes was independent of the high-order chromatin structure of autosomes in both FGSCs and SSCs. Considering that female embryonic stem cells (fESCs) have two activated X chromosomes (Xa), whereas one X chromosome was inactivated in FGSCs, we analyzed the correlation of the PC1 score of the X chromosome in FGSCs, SSCs, and fESCs.[5] We found that the X chromosome in FGSCs was more highly correlated with the X chromosome in SSCs than it was with the X chromosome in fESCs (Fig. 1F). This finding suggests that the X chromosome was similar between FGSCs and SSCs, probably because one of the X chromosomes was inactivated (Xi) in FGSCs. To validate the inactivation of the X chromosome in FGSCs, we performed RNA FISH for *Xist* in FGSCs. *Xist* is a long noncoding RNA that can orchestrate the silencing process of the X chromosome and its expression reflects the inactivation of X chromosome. We used a red-labeled *Xist* probe to confirm the inactivation of the X chromosome of in vitro cultured FGSCs and blue-labeled DAPI to stain the nuclei of the FGSCs. The results showed that one X chromosome was inactivated in FGSCs (Fig. S5A, B), which confirmed that the FGSCs had one inactive X chromosome and one activate X chromosome, and suggested that the high-order chromatin structure could be different from that for two active X chromosomes. To identify the differences between active and inactive X chromosomes, we deconvoluted the Hi-C data of these chromosomes from FGSCs (Fig. 1G). As expected, the X chromosome was separated by a region that contained the DXZ4 macrosatellite (which reportedly plays a crucial role in shaping the Xi structure) into two parts in FGSCs, as well as in deconvoluted Xi, which was not the case in SSCs (Fig. 1G). This finding demonstrated that one of the X chromosomes in FGSCs was inactivated. In deconvoluted Xi, the long-range contacts were attenuated for intra- and inter-TADs (Fig. 1G). By comparison of the contact probability against genomic distance between Xa and Xi, we found the contact frequency of Xi was decreased more dramatically at a distance of >60 Mb (Fig. S6A). It showed Xi had reduced long-range chromatin interactions, suggesting Xi could be more condensed than Xa. To further explore the condensation structure of X chromosome, we constructed the 3D model in Xa and Xi, respectively. The simulated physical 3D model of Xa displayed a more elongated formation than Xi, indicating that Xi was more condensed than Xa (Fig. 1H). Furthermore, we colored the physical model with the compartment status to investigate the difference between Xa and Xi. The result showed Xa had smaller and more dispersed compartments, while Xi had more concentrated compartments, suggesting Xa had more complex compartmentalization which possibly was contributed to the gene regulation (Fig. 1H). Next, we investigated the structure of the region containing *Xist*, a key factor for inactivation of the X chromosome. Notably, the *Xist* region was similar in FGSCs and SSCs, whereas, in deconvolved Xi, the *Xist* region lost most of the long-range contacts and retained a sub-TAD-like structure (Fig. S6B). Together, our results suggest that one of the X chromosomes was inactivated in FGSCs.

Author contributions

G.T. devised this study and performed the ChIP-seq, RNA-seq and Hi-C data analysis and wrote the manuscript. J.W. and J.L. supervised the experiment work and devised this study.

Funding

This work was supported by National Nature Science Foundation of China (No. 81720108017, 31871329), the National Major Scientific Instruments and Equipment Development Project, National Nature Science Foundation of China (No. 61827814) and the China Postdoctoral Science Foundation (No. 2021M692081).

Conflict of interests

The authors declare no conflict of interests.

Appendix A. Supplementary data

Supplementary data to this article can be found online at https://doi.org/10.1016/j.gendis.2022.09.003.

References

1. Zhang XL, Wu J, Wang J, et al. Integrative epigenomic analysis reveals unique epigenetic signatures involved in unipotency of mouse female germline stem cells. *Genome Biol*. 2016; 17(1):162.
2. Liu Y, Giannopoulou EG, Wen D, et al. Epigenetic profiles signify cell fate plasticity in unipotent spermatogonial stem and progenitor cells. *Nat Commun*. 2016;7:11275.
3. Tian GG, Zhao X, Hou C, et al. Integrative analysis of the 3D genome structure reveals that CTCF maintains the properties of mouse female germline stem cells. *Cell Mol Life Sci*. 2022; 79(1):22.
4. Huynh KD, Lee JT. X-chromosome inactivation: a hypothesis linking ontogeny and phylogeny. *Nat Rev Genet*. 2005;6(5): 410–418.

5. Marks H, Kerstens HH, Barakat TS, et al. Dynamics of gene silencing during X inactivation using allele-specific RNA-seq. *Genome Biol*. 2015;16(1):149.

Geng G. Tian [a], Jing Li [b,**], Ji Wu [a,c,*]

[a] *Renji Hospital, Key Laboratory for the Genetics of Developmental & Neuropsychiatric Disorders (Ministry of Education), Bio-X Institutes, School of Medicine, Shanghai Jiao Tong University, Shanghai 200240, China*
[b] *Department of Bioinformatics and Biostatistics, School of Life Sciences and Biotechnology, Shanghai Jiao Tong University, Shanghai 200240, China*
[c] *Key Laboratory of Fertility Preservation and Maintenance of Ministry of Education, Ningxia Medical University, Yinchuan, Ningxia 750004, China*

*Corresponding author. Renji Hospital, Key Laboratory for the Genetics of Developmental & Neuropsychiatric Disorders (Ministry of Education), Bio-X Institutes, School of Medicine, Shanghai Jiao Tong University, Shanghai 200240, China.

**Corresponding author.
E-mail addresses: jing.li@sjtu.edu.cn (J. Li), jiwu@sjtu.edu.cn (J. Wu)

7 January 2022
Available online 20 September 2022